

Stable multi-ring and rotating solitons in two-dimensional spin-orbit coupled Bose-Einstein condensates with a radially-periodic potential

Yaroslav V. Kartashov^{1,2} and Dmitry A. Zezyulin³

¹*ICFO-Institut de Ciències Fòniques, The Barcelona Institute of Science and Technology, 08860 Castelldefels (Barcelona), Spain*

²*Institute of Spectroscopy, Russian Academy of Sciences, Troitsk, Moscow, 108840, Russia*

³*ITMO University, St. Petersburg 197101, Russia*

(Dated: March 28, 2019)

We consider two-dimensional spin-orbit coupled atomic Bose-Einstein condensate in a radially-periodic potential. The system supports different types of stable self-sustained states including radially-symmetric vorticity-carrying modes with different topological charges in two spinor components that may have multiring profiles and at the same time remain remarkably stable for repulsive interactions. Solitons of the second type show persistent rotation with constant angular frequency. They can be stable for both repulsive and attractive interatomic interactions. Due to inequivalence between clockwise and counterclockwise rotation directions introduced by spin-orbit coupling, the properties of such solitons strongly differ for positive and negative rotation frequencies. Collision of solitons located in the same or different rings is accompanied by change of the rotation frequency that depends on the phase difference between colliding solitons.

Nonlinear wave phenomena in atomic Bose-Einstein condensates (BECs) attract considerable attention [1–3]. Depending on the sign of the interatomic interactions one can observe the formation in BEC of bright or dark solitons. Their properties critically depend on the dimensionality of the condensate, since multidimensional states in BECs with attractive and repulsive interatomic interactions may be prone, respectively, to collapse or various snaking instabilities. Bright solitons can be obtained in a Bose-Fermi mixture of degenerate gases, even if interatomic interaction in the Bose component are repulsive [4, 5]. Another powerful approach to stabilization of multidimensional states in BEC relies on the external potentials, including periodic ones [6–8]. Besides conventional states that do not change upon evolution [9], such potentials, when they are radially-symmetric [10–12], support stable solitons exhibiting persistent rotation. The properties of such solitons in single-component BECs do not depend on the rotation direction.

This situation may change dramatically in spin-orbit coupled two-component condensates (SO-BECs) which are attracting steadily growing interest. SO-BECs, representing a mixture of different states of the same atomic species, were recently used for demonstration of coupling between pseudospin degree of freedom and spatial structure of the condensate [13–15]. SO-BECs offer a versatile platform for investigation of the nonlinear phenomena in the presence of synthetic fields [16] and gauge potentials [17], see review [18]. SO coupling notably modifies dispersion of the system [19, 20], it may break Galilean invariance [14, 21], and substantially impacts properties of one- [22, 23] and multidimensional [24, 25] solitons in the free space. Especially intriguing is the impact of SO coupling on BEC in the external potentials, where possible symmetries of self-sustained states and their evolution dynamics are determined by the symmetry of the po-

tential. It was studied for solitons on a ring [26] and in harmonic trap [27], in toroidal traps [28], Bessel [29], and periodic [30] lattices.

While it was shown for radially-symmetric potentials [28] that SO coupling notably enriches two-dimensional soliton families and leads to appearance of azimuthal density modulations, the most important and unexpected manifestation of this effect, consisting in breakup of equivalence of two rotation directions (clockwise and counterclockwise) for solitons, was not demonstrated in atomic BECs. This is also the case for literature [31] on trapped SO-BEC under rotation that studies condensate transformation for one sign of the rotation frequency. While this inequivalence has been encountered in polariton condensates in a circular geometry [32], polaritons represent an essentially non-equilibrium system, where dominating interactions are repulsive, and where effective SO coupling has completely different physical origin (it stems from TE-TM splitting) and is relatively weak. Thus, the question arises, whether this phenomenon exists in *conservative* atomic BECs where SO coupling is *considerable* and where interactions can be both *repulsive* and *attractive*.

Here we first introduce SO coupling into BEC in a radially-periodic potential and show that in the repulsive case it supports stable *multiring* vortex solitons carrying different topological charges in two components. Such structures have never been obtained in SO-BECs before and are in clear contrast to previously encountered azimuthally modulated patterns. Second, we show that radially-periodic potentials support stable *rotating multipole* states for repulsive nonlinearity and *crescent-like fundamental* states for attractive nonlinearity, reminiscent of azimuthons [33], that feature unexpected dependence not only on modulus, but also on *sign* of the rotation frequency clearly illustrating inequivalence of two

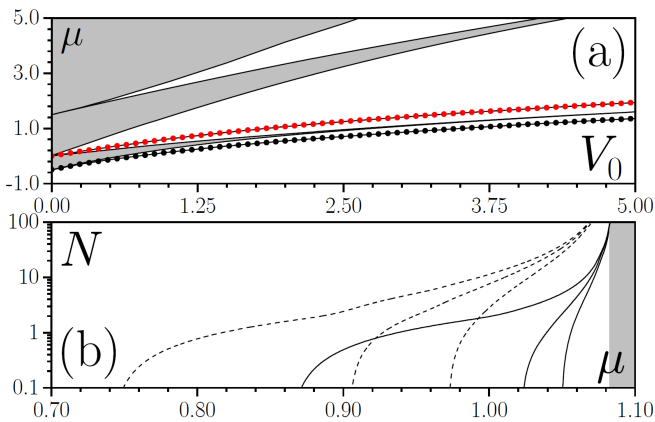


FIG. 1. (a) Bands (gray) and gaps (white) of radial potential and eigenvalues of linear modes (lines with circles) with $m_{\pm} = (-1, 0)$ residing in the first potential minimum. (b) N vs μ for simplest soliton families with $m_{\pm} = (-1, 0)$ (solid lines) and $m_{\pm} = (-2, -1)$ (dashed lines) in the semi-infinite gap at $\sigma = 1$. For each m_{\pm} set three families are shown with density maxima in the first, second, and third minima of $V(r)$.

azimuthal directions. Third, we study interactions of rotating solitons for attractive nonlinearity and show that they lead to change in rotation frequency that also depends on soliton phase difference.

Meanfield dynamics of two-dimensional BEC is described by the normalized Gross-Pitaevskii equations with Rashba SO coupling [34]:

$$i\partial_t\psi_{\pm} = -(1/2)(\partial_x^2 + \partial_y^2)\psi_{\pm} + V(r)\psi_{\pm} \pm \beta(\partial_x \mp i\partial_y)\psi_{\mp} + \sigma(|\psi_{\pm}|^2 + |\psi_{\mp}|^2)\psi_{\pm}. \quad (1)$$

Here $(\psi_+, \psi_-)^T$ is the spinor macroscopic wavefunction; t and x, y are dimensionless time and spatial coordinates, scaled to characteristic time \hbar/\mathcal{E}_0 and spatial scale R_0 , respectively; $\mathcal{E}_0 = \hbar^2/mR_0^2$ is characteristic energy; m is the atomic mass; β characterizes the strength of SO coupling that can be considerable; $\sigma = \pm 1$ corresponds to repulsive/attractive interactions; $V(r) = 2V_0 \cos^2(r)$ is the radially-periodic potential with depth $2V_0$ measured in units of \mathcal{E}_0 (hereafter r and θ are the polar radius and angle); in what follows, we set $V_0 = 3$. The radially-periodic potential can be created using a cylindrical laser beam whose amplitude is modulated with a patterned mask (the conical diffraction of the beam with the waist diameter $\simeq 100 \mu\text{m}$ will be negligible for the tightly-confined disk-shaped condensate with thickness $\simeq 2 \mu\text{m}$ [12]). SO coupling is created by laser beams which couple different states of ^{87}Rb atoms (the case of repulsive interactions) or ^7Li atoms (attractive interactions); its strength can be varied in a broad range depending on laser configurations [20]; see also [13–15, 22] for detailed discussion on implementation of SO-BECs.

The simplest states are radially-symmetric solitons $\psi_{\pm} = u_{\pm}(r)e^{-i\mu t + im_{\pm}\theta}$, where m_{\pm} are the topological

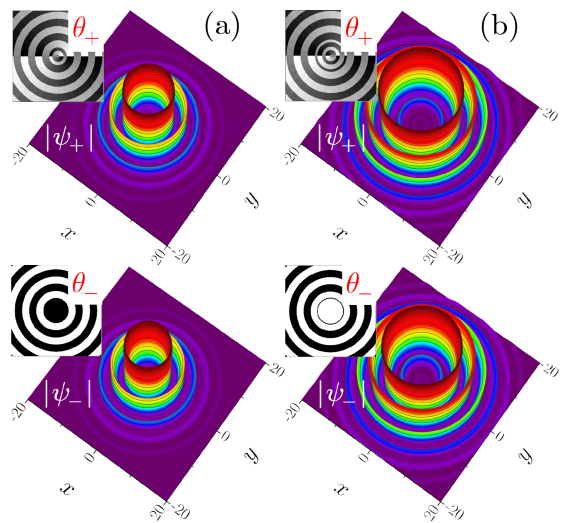


FIG. 2. Modulus and phase (insets) distributions in $m_{\pm} = (-1, 0)$ radially-symmetric solitons from different families, with $\mu = 1.05$ (a) and $\mu = 1.06$ (b) at $\beta = 1, \sigma = 1$.

charges satisfying the condition $m_- = m_+ + 1$ that is due to the linear spin-orbit coupling preserving the total angular momentum, μ is the chemical potential, and u_{\pm} are real-valued. We search for localized solutions carrying finite norm $N = 2\pi \int_0^{\infty} r(u_+^2 + u_-^2)dr$ (which is proportional to the total number of particles in the condensate). At $r \rightarrow \infty$ the effect of nonlinear terms becomes negligible, and the intervals of chemical potential, where localized states can exist, are determined by the eigenvalue problem $\mu u_{\pm} = -(1/2)\partial_r^2 u_{\pm} + V(r)u_{\pm} \pm \beta\partial_r u_{\mp}$. This problem is π -periodic and features the bandgap spectrum shown in Fig. 1(a). Localized nonlinear modes — radial gap solitons — exist for μ values lying in the spectral gaps [white regions in Fig. 1(a)]. However, in contrast to usual gap solitons, nonlinear modes in the radially-periodic potential remain completely localized also in the small-amplitude limit, when the corresponding norm vanishes, $N \rightarrow 0$. This feature is readily visible from Fig. 1(b), where we plot several dependencies $N(\mu)$ for nonlinear modes with topological charges $m_{\pm} = (-1, 0)$ (solid curves) and $m_{\pm} = (-2, -1)$ (dashed curves) and density maxima located in radial minima of the potential at $r = \pi/2, 3\pi/2$, and $5\pi/2$. In the limit $N \rightarrow 0$, each of these soliton families bifurcates from appropriate localized linear mode with chemical potential μ from the gap. Eigenvalues of linear modes in the semi-infinite and first finite gaps from which the simplest solitons with density maximum at $r = \pi/2$ bifurcate are shown in Fig. 1(a) by lines with circles. In spite of the repulsive interactions, $\sigma = 1$, families shown in Fig. 1(b) belong to the semi-infinite gap (which is possible due to the radial periodicity of the trap). When μ approaches the edge of the gap, vortex modes acquire well-pronounced multir-

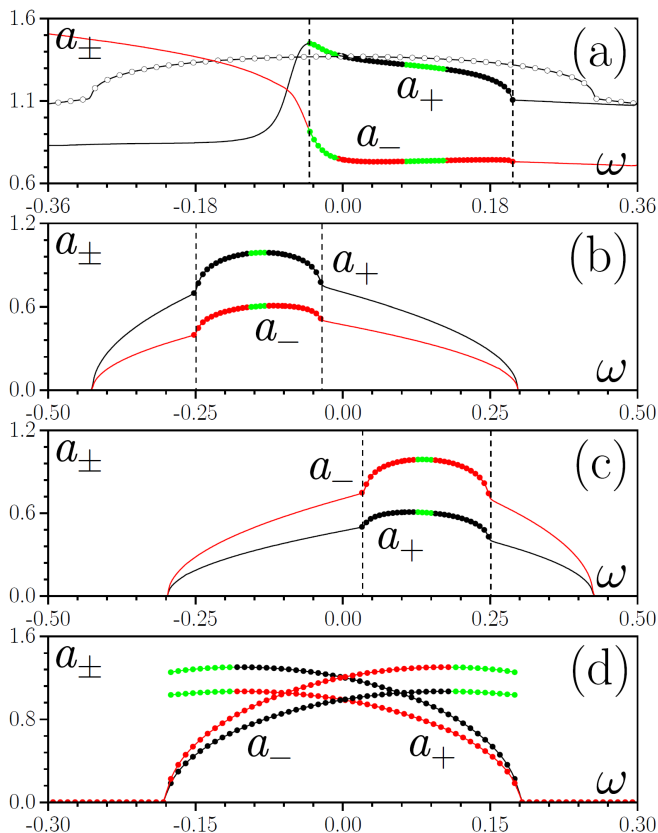


FIG. 3. Lines with solid circles show amplitudes a_{\pm} of ψ_{\pm} components in rotating dipole (a) and quadrupole (b),(c) solitons versus ω at $\mu = 3$, $\beta = 0.5$, $\sigma = 1$. Line with open circles in (a) shows $a_+(\omega)$ dependence at $\beta = 0$. Dominating component is ψ_+ in (b) and ψ_- in (c). Thin lines in (b),(c) correspond to radially-symmetric states. (d) $a_{\pm}(\omega)$ in rotating fundamental solitons at $\mu = 0.6$, $\beta = 0.5$, $\sigma = -1$. Green circles indicate unstable branches.

ing structure (see examples in Fig. 2). Standard linear stability analysis [34, 35] and direct integration of Eq. (1) indicate stability of all vortex states shown in Fig. 1(b) and Fig. 2, in spite of their complex multiring shapes. Stable radially-symmetric vortex solitons can be found not only in the semi-infinite gap but also in finite spectral gaps, as shown in Figs. 3 and 5.

Now we turn to rotating states without radial symmetry. They are sought as $\psi_{\pm} = u_{\pm}(x', y')e^{-i(\mu \pm \omega/2)t}$ in the rotating frame $x' = x\cos(\omega t) + y\sin(\omega t)$, $y' = y\cos(\omega t) - x\sin(\omega t)$, where complex functions u_{\pm} solve (we further omit primes):

$$\begin{aligned} \mu u_{\pm} = & -(1/2)(\partial_x^2 + \partial_y^2)u_{\pm} + V(r)u_{\pm} \pm \beta(\partial_x \mp i\partial_y)u_{\mp} \\ & + \sigma(|u_{\pm}|^2 + |u_{\mp}|^2)u_{\pm} + i\omega(x\partial_y - y\partial_x)u_{\pm} \mp (\omega/2)u_{\pm}. \end{aligned} \quad (2)$$

Rotation with frequency ω results in penultimate Coriolis term in Eq. (2), while the last term originates from the assumed form of time-dependence in ψ_{\pm} that is required to eliminate time-dependence in SO coupling term

in the rotating frame. Equation (2) admits a variety of rotating solitons residing in different radial minima of the potential. We start with repulsive nonlinearity ($\sigma = 1$) and consider simplest solitons from the first minimum at $r = \pi/2$ with chemical potentials μ from the first finite gap. At $\beta, \omega = 0$ they represent dipole (two out-of-phase spots in u_+ or u_- component) and quadrupole (four spots in u_+ or u_- with π phase jumps) solitons. At $\beta = 0$ increasing or decreasing rotation frequency smoothly transforms multipole states into radially-symmetric vortices. Dependence of amplitude $a_{\pm} = \max|u_{\pm}(x, y)|$ of soliton components on ω is symmetric in this case, see line with open circles in Fig. 3(a) for dipole solitons. Thus at $\beta = 0$ the properties of such solitons do not depend on the rotation direction. This picture changes qualitatively in the presence of SO coupling: the dependence $a_{\pm}(\omega)$ becomes asymmetric at $\beta \neq 0$. For dipole solitons with dominating u_+ component the entire domain of existence of rotating solitons shifts toward positive frequency values [lines with solid circles in Fig. 3(a) between two vertical dashed lines marking the border of the existence domain]. For dipole states with dominating u_- component the existence domain shifts toward negative frequencies. The existence domains for rotating solitons with different dominating components are thus mirror-symmetric with respect to $\omega = 0$, as illustrated for quadrupole solitons in Figs. 3(b,c). Inequivalence of azimuthal directions in SO-BEC illustrated by Fig. 3 is one of the central results of this Letter. For characteristic scale of $R_0 = 2 \mu\text{m}$, dimensionless frequency $\omega = 0.25$ corresponds to rotation periods of 137 ms in ^{87}Rb and 11 ms in ^7Li condensate [34], that is well below condensate lifetime available in the state-of-the-art experiments.

Variation of rotation frequency causes notable shape transformations. Examples of modulus $|\psi_{\pm}|$ and phase θ_{\pm} distributions for different frequencies in dipole and quadrupole solitons are shown in Fig. 4(a-d). On the right edge of the existence domain in ω [Fig. 4(a)] such dipoles turn into $m_{\pm} = (-1, 0)$ radially-symmetric vortices, while on the left edge [Fig. 4(b)] they become strongly modulated and dynamically unstable. Quadrupole solitons transform into $m_{\pm} = (-2, -1)$ vortices on the right edge [Fig. 4(c)] of the existence domain and into $m_{\pm} = (+2, +3)$ vortices on its left edge [Fig. 4(d)]. Transformation of phase distribution upon variation of ω resembles topological charge flipping [36].

Families of radially-symmetric states into which rotating solitons transform can be further continued in ω as shown by thin lines in Fig. 3. At fixed ω and $\sigma = 1$ all rotating solitons (lines with circles) bifurcate with increase of chemical potential μ from radially-symmetric solitons (thin lines), which emanate from corresponding linear modes, as shown in Fig. 5. The charge of the state, from which bifurcation occurs, is determined by ω : it is $(-1, 0)$ in Fig. 5(a) and $(-2, -1)$ in Fig. 5(b). When μ increases and approaches the border of the first gap, ro-

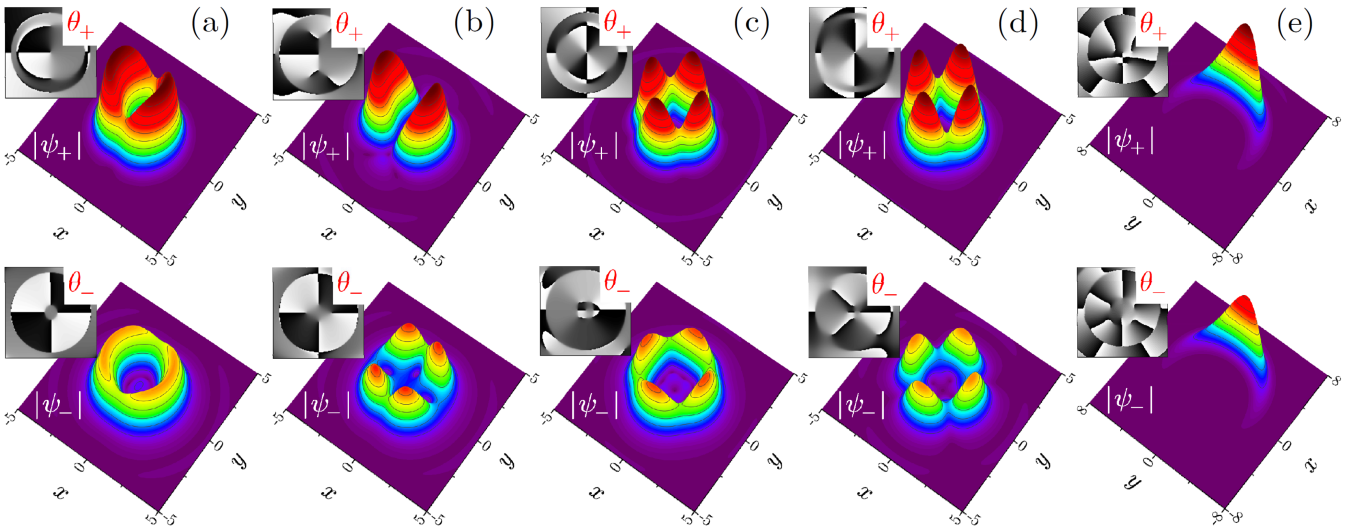


FIG. 4. Modulus and phase (insets) distributions in dipole solitons with (a) $\omega = 0.13$, (b) $\omega = -0.04$, and quadrupole solitons with (c) $\omega = -0.06$, (d) $\omega = -0.22$ at $\mu = 3$, $\beta = 0.5$, $\sigma = 1$, and fundamental solitons with (e) $\omega = 0.15$ at $\mu = 0.6$, $\beta = 0.5$, $\sigma = -1$. In all cases ψ_+ is a dominating component; $|\psi_+|$ and $|\psi_-|$ distributions are plotted with the same scale in each soliton.

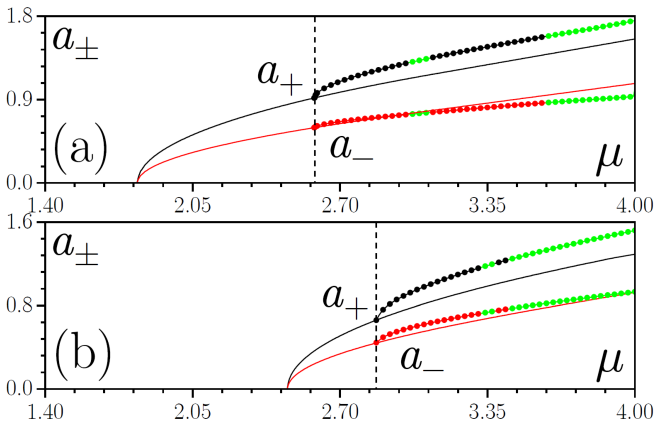


FIG. 5. Lines with circles: $a_{\pm}(\mu)$ dependencies for (a) rotating dipole soliton with $\omega = 0.12$ and (b) quadrupole soliton with $\omega = -0.06$ at $\beta = 0.5$, $\sigma = 1$. Thin lines: $a_{\pm}(\mu)$ for radially-symmetric $m_{\pm} = (-1, 0)$ (a) and $m_{\pm} = (-2, -1)$ (b) states. Green circles indicate unstable branches.

tating modes develop multiring structure and eventually delocalize.

In contrast to polariton condensates, both dipole and quadrupole rotating solitons in repulsive SO-BECs are dynamically stable in wide parameter regions even for β values comparable to 1. Stability was also tested by modeling the evolution of slightly perturbed states up to huge times $t \sim 10^4$ in Eq. (1). Instability domains are indicated by green circles in Figs. 3 and 5, while black/red circles correspond to stable branches. Rotating solitons are always stable in the parameter domains adjacent to bifurcation points from radially-symmetric solitons. Ex-

amples of evolutions with stable and unstable rotations are given in Figs. 6(a,b,c).

SO-BEC with attractive nonlinearity ($\sigma = -1$) supports simpler fundamental rotating solitons with unusual crescent-like shapes, see Fig. 4(e). Such solitons exist in semi-infinite gap and resemble whispering-gallery modes [37]. The dependencies of amplitudes a_{\pm} of such solitons are also strongly asymmetric in rotation frequency ω [Fig. 3(d)]: at one border of the existence domain in ω soliton gradually expands along the entire ring where it resides (soliton is stable in broad domain adjacent to this border), while on another border one observes development of unstable multiring structure. Since such solitons are better localized than their counterparts in repulsive condensate, one can study their collision in the same [Fig. 6(d₁-d₃)] or in different [Fig. 6(e₁-e₃)] rings. Taking two solitons with opposite rotation frequencies ω and equal norms (μ values), one unexpectedly finds that after collision [Fig. 6(d₂)] both solitons *accelerate* [compare input in Fig. 6(d₁) with output in Fig. 6(d₃) after $t = 2\pi/\omega$], i.e., collision in this system changes rotation frequencies. Moreover, the variation in ω depends on phase difference between colliding solitons. Thus, when two solitons with opposite frequencies at $t = 0$ collide in different rings [Fig. 6(e₁-e₃)] the outer (inner) soliton accelerates (decelerates) upon consecutive collisions for in-phase solitons [Fig. 6(e₂)], while for out-of-phase states this tendency reverses [Fig. 6(e₃)] leading to different final density distributions.

Summarizing, we demonstrated that SO coupling in trapped BEC with repulsive or attractive interaction breaks the equivalence of two rotation directions. Rotating solitons feature strongly asymmetric ex-

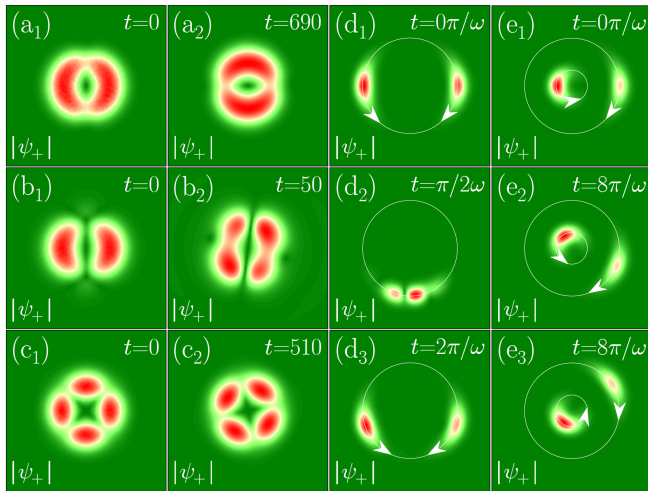


FIG. 6. Stable (a,c) and unstable (b) evolution of rotating dipole and quadrupole solitons at (a) $\omega = 0.13$, (b) $\omega = -0.04$, (c) $\omega = -0.22$ and $\mu = 3$, $\beta = 0.5$, $\sigma = 1$. Interaction of two fundamental solitons in the same (d₁-d₃) and in different (e₁-e₃) rings at $\mu = 0.6$, $\beta = 0.5$, $\sigma = -1$. Solitons are in-phase in (d₁-d₃) and (e₂) and out-of-phase in (e₃) and have opposite rotation frequencies $\omega = \pm 1$.

istence domains in rotation frequency and feature non-conventional collisional behaviors involving their acceleration/deceleration determined by the phase difference between solitons.

Acknowledgments. The research of D.A.Z. was supported by megaGrant No. 14.Y26.31.0015 of the Ministry of Education and Science of Russian Federation and by Government of Russian Federation (Grant 08-08).

[1] C. Pethick and H. Smith, *Bose-Einstein Condensation in Dilute Gases* (Cambridge University Press: Cambridge, 2002); L. Pitaevskii and S. Stringari, *Bose-Einstein condensation* (Clarendon Press, Oxford, 2003).

[2] P. G. Kevrekidis, D. J. Frantzeskakis, and R. Carretero-González (Eds.), *Emergent nonlinear phenomena in Bose-Einstein condensates*, Springer Series on Atomic, Optical, and Plasma Physics, **45** (Springer, 2008).

[3] A. L. Fetter, Rotating trapped Bose-Einstein condensates, *Rev. Mod. Phys.* **81**, 647 (2009).

[4] T. Karpiuk, M. Brewczyk, S. Ospelkaus-Schwarzer, K. Bongs, M. Gajda, and K. Rzȃżewski, Soliton Trains in Bose-Fermi Mixtures, *Phys. Rev. Lett.* **93**, 100401 (2004); J. Santhanam, V. M. Kenkre, and V. V. Konotop, Solitons of Bose-Fermi mixtures in a strongly elongated trap, *Phys. Rev. A* **73**, 013612 (2006).

[5] B.J. DeSalvo, K. Patel, G. Cai, C. Chin, Fermion-Mediated Interactions Between Bosonic Atoms, arXiv:1808.07856.

[6] V. A. Braznyi and V. V. Konotop, Theory of nonlinear matter waves in optical lattices, *Mod. Phys. Lett. B* **18**, 627 (2004); Y. V. Kartashov, B. A. Malomed, and L.

Torner, Solitons in nonlinear lattices, *Rev. Mod. Phys.* **83**, 247 (2011).

[7] O. Morsch and M. Oberthaler, Dynamics of Bose-Einstein condensates in optical lattices, *Rev. Mod. Phys.* **78**, 179 (2006).

[8] R. Carretero-González, D. J. Frantzeskakis, and P. G. Kevrekidis, Nonlinear waves in Bose-Einstein condensates: physical relevance and mathematical techniques, *Nonlinearity* **21**, R139 (2008).

[9] E. A. Ostrovskaya and Y. S. Kivshar, Matter-wave gap solitons in atomic band-gap structures, *Phys. Rev. Lett.* **90**, 160407 (2003); B. Eiermann, T. Anker, M. Albiez, M. Taglieber, P. Treutlein, K.-P. Marzlin, and M. K. Oberthaler, Bright Bose-Einstein gap solitons of atoms with repulsive interaction, *Phys. Rev. Lett.* **92**, 230401 (2004); E. A. Ostrovskaya and Y. S. Kivshar, Matter-wave gap vortices in optical lattices, *Phys. Rev. Lett.* **93**, 160405 (2004).

[10] Y. V. Kartashov, V. A. Vysloukh, and L. Torner, Rotary solitons in Bessel optical lattices, *Phys. Rev. Lett.* **93**, 093904 (2004); Y. V. Kartashov, V. A. Vysloukh, L. Torner, Stable ring-profile vortex solitons in Bessel optical lattices, *Phys. Rev. Lett.* **94**, 043902 (2005); X. S. Wang, Z. G. Chen, P. G. Kevrekidis, Observation of discrete solitons and soliton rotation in optically induced periodic ring lattices, *Phys. Rev. Lett.* **96**, 083904 (2006).

[11] A. V. Carpentier and H. Michinel, A ring accelerator for matter-wave solitons, *EPL* **78**, 10002 (2007); C. Ryu, M. F. Andersen, P. Clad, V. Natarajan, K. Helmerson, and W. D. Phillips, Observation of persistent flow of a Bose-Einstein condensate in a toroidal trap, *Phys. Rev. Lett.* **99**, 260401 (2007).

[12] B. Baizakov, B. A. Malomed, and M. Salerno, Matter-wave solitons in radially periodic potentials, *Phys. Rev. E* **74**, 066615 (2006).

[13] Y. J. Lin, K. Jiménez-García, and I. B. Spielman, Spin-orbit-coupled Bose-Einstein condensates, *Nature* **471**, 83 (2011).

[14] C. Hamner, Y. Zhang, M.A. Khamehchi, M. J. Davis, and P. Engels, Spin-orbit-coupled Bose-Einstein condensates in a one-dimensional optical lattice, *Phys. Rev. Lett.* **114**, 070401 (2015).

[15] Z. Wu, L. Zhang, W. Sun, X. T. Xu, B. Z. Wang, S. C. Ji, Y. Deng, S. Chen, X. J. Liu, and J. W. Pan, Realization of two-dimensional spin-orbit coupling for Bose-Einstein condensates, *Science* **354**, 83 (2016).

[16] Y.-J. Lin, R. L. Compton, K. Jimenez-Garcia, J. V. Porto, and I. B. Spielman, Synthetic magnetic fields for ultracold neutral atoms, *Nature* **462**, 628 (2009).

[17] J. Ruseckas, G. Juzeliunas, P. Öhberg, and M. Fleischhauer, Non-Abelian gauge potentials for ultracold atoms with degenerate dark states, *Phys. Rev. Lett.* **95**, 010404 (2005); T.-L. Ho and S. Zhang, Bose-Einstein condensates with spin-orbit interaction, *Phys. Rev. Lett.* **107**, 150403 (2011); Y.-J. Lin, R. L. Compton, A. R. Perry, W. D. Phillips, J. V. Porto, and I. B. Spielman, Bose-Einstein condensate in a uniform light-induced vector potential, *Phys. Rev. Lett.* **102**, 130401 (2009).

[18] J. Dalibard, F. Gerbier, G. Juzeliūnas, and P. Öhberg, Colloquium: Artificial gauge potentials for neutral atoms, *Rev. Mod. Phys.* **83**, 1523 (2011).

[19] C. Wang, C. Gao, C.-M. Jian, and H. Zhai, Chunji Wang, Chao Gao, Chao-Ming Jian, and Hui Zhai, Spin-orbit cou-

- pled spinor Bose-Einstein condensates, *Phys. Rev. Lett.* **105**, 160403 (2010); S. Sinha, R. Nath, and L. Santos, Trapped two-dimensional condensates with synthetic spin-orbit coupling, *Phys. Rev. Lett.* **107**, 270401 (2011); H. Hu, B. Ramachandhran, H. Pu, and X.-J. Liu, Spin-orbit coupled weakly interacting Bose-Einstein condensates in harmonic traps, *Phys. Rev. Lett.* **108**, 010402 (2012); Y. Li, G. I. Martone, L. P. Pitaevskii, and S. Stringari, Superstripes and the excitation spectrum of a spin-orbit-coupled Bose-Einstein condensate, *Phys. Rev. Lett.* **110**, 235302 (2013).
- [20] Y. Zhang, L. Mao, and C. Zhang, Mean-field dynamics of spin-orbit-coupled Bose-Einstein condensates, *Phys. Rev. Lett.* **108**, 035302 (2012).
- [21] Q. Zhu, C. Zhang, and B. Wu, Exotic superfluidity in spin-orbit coupled Bose-Einstein condensates, *EPL* **100**, 50003 (2012).
- [22] V. Achilleos, D. J. Frantzeskakis, P. G. Kevrekidis, and D. E. Pelinovsky, Matter-wave bright solitons in spin-orbit coupled Bose-Einstein condensates, *Phys. Rev. Lett.* **110**, 264101 (2013).
- [23] Y. Xu, Y. Zhang, and B. Wu, Bright solitons in spin-orbit-coupled Bose-Einstein condensates, *Phys. Rev. A* **87**, 013614 (2013); Y. V. Kartashov, V. V. Konotop, and D. A. Zezyulin, Bose-Einstein condensates with localized spin-orbit coupling: Soliton complexes and spinor dynamics, *Phys. Rev. A* **90**, 063621 (2014).
- [24] H. Sakaguchi, B. Li, B. A. Malomed, Creation of two-dimensional composite solitons in spin-orbit-coupled self-attractive Bose-Einstein condensates in free space, *Phys. Rev. E* **89**, 032920 (2014); X. Jiang, Z. Fan, Z. Chen, W. Pang, Y. Li, and B. A. Malomed, Two-dimensional solitons in dipolar Bose-Einstein condensates with spin-orbit coupling, *Phys. Rev. A* **93**, 023633 (2016).
- [25] Y.-C. Zhang, Z.-W. Zhou, B. A. Malomed, and H. Pu, Stable solitons in three-dimensional free space without the ground state: Self-trapped Bose-Einstein condensates with spin-orbit coupling, *Phys. Rev. Lett.* **115**, 253902 (2015).
- [26] O. Fialko, J. Brand, and U. Zulicke, Soliton magnetization dynamics in spin-orbit-coupled Bose-Einstein condensates, *Phys. Rev. A* **85**, 051605(R) (2012).
- [27] D. A. Zezyulin, R. Driben, V. V. Konotop, and B. A. Malomed, Nonlinear modes in binary bosonic condensates with pseudo-spin-orbital coupling, *Phys. Rev. A* **88**, 013607 (2013);
- [28] E. Ö. Karabulut, F. Malet, A. L. Fetter, G. M. Kavoulakis, and S. M. Reimann, Spin-orbit-coupled Bose-Einstein-condensed atoms confined in annular potentials, *New J. Phys.* **18**, 015013 (2016); X.-F. Zhang, M. Kato, W. Han, S.-G. Zhang, and H. Saito, Spin-orbit-coupled Bose-Einstein condensates held under a toroidal trap, *Phys. Rev. A* **95**, 033620 (2017); A. C. White, Y. Zhang, and T. Busch, Odd-petal-number states and persistent flows in spin-orbit-coupled Bose-Einstein condensates, *Phys. Rev. A* **95**, 041604(R) (2017).
- [29] H. Li, S.-L. Xu, M. R. Belić, and J.-X. Cheng, Three-dimensional solitons in Bose-Einstein condensates with spin-orbit coupling and Bessel optical lattices, *Phys. Rev. A* **98**, 033827 (2018).
- [30] Y. V. Kartashov, V. V. Konotop, and F. K. Abdullaev, Gap solitons in a spin-orbit-coupled Bose-Einstein condensate, *Phys. Rev. Lett.* **111**, 060402 (2013); V. E. Lobanov, Y. V. Kartashov, and V. V. Konotop, Fundamental, multipole, and half-vortex gap solitons in spin-orbit coupled Bose-Einstein condensates, *Phys. Rev. Lett.* **112**, 180403 (2014); Y. Zhang, Y. Xu, and T. Busch, Gap solitons in spin-orbit-coupled Bose-Einstein condensates in optical lattices, *Phys. Rev. A* **91**, 043629 (2015); M. Salerno, F. K. Abdullaev, G. A. Gammal, and L. Tomio, Tunable spin-orbit-coupled Bose-Einstein condensates in deep optical lattices, *Phys. Rev. A* **94**, 043602 (2016).
- [31] X.-Qi. Xu and J. H. Han, Spin-orbit coupled Bose-Einstein condensate under rotation, *Phys. Rev. Lett.* **107**, 200401 (2011); J. Radić, T. A. Sedrakyan, I. B. Spielman, and V. Galitski, Vortices in spin-orbit-coupled Bose-Einstein condensates, *Phys. Rev. A* **84**, 063604 (2011); X.-F. Zhou, J. Zhou, and C. Wu, Vortex structures of rotating spin-orbit-coupled Bose-Einstein condensates, *Phys. Rev. A* **84**, 063624 (2011); H. Sakaguchi and K. Umeda, *J. Phys. Soc. Jpn.* **85**, 064402 (2016); J.-G. Wang, L.-L. Xu, and S.-J. Yang, Ground-state phases of a rotating spin-orbit-coupled Bose-Einstein condensate in an optical lattice, *EPL* **120**, 20006 (2017); Z.-M. He, X.-F. Zhang, M. Kato, W. Han, H. Saito, Stationary states and rotational properties of spin-orbit-coupled Bose-Einstein condensates held under a toroidal trap, *Phys. Lett. A* **382**, 1690 (2018).
- [32] D. A. Zezyulin, Y. V. Kartashov, D. V. Skryabin, and I. A. Shelykh, Spin-Orbit Coupled Polariton Condensates in a Radially Periodic Potential: Multiring Vortices and Rotating Solitons, *ACS Photonics* **5**, 3634 (2018).
- [33] A. S. Desyatnikov, A. A. Sukhorukov, and Y. S. Kivshar, Azimuthons: Spatially modulated vortex solitons, *Phys. Rev. Lett.* **95**, 203904 (2005); V. M. Lashkin, Two-dimensional multisolitons and azimuthons in Bose-Einstein condensates, *Phys. Rev. A* **77**, 025602 (2008).
- [34] See Supplemental Material for the Gross-Pitaevskii equation written in physical units and details of stability analysis.
- [35] A. L. Fetter and A. A. Svidzinsky, Vortices in a trapped dilute Bose-Einstein condensate, *J. Phys.: Condens. Matter* **13**, R135-R194 (2001).
- [36] A. Bezryadina, D. N. Neshev, A. S. Desyatnikov, J. Young, Z. Chen, and Y. S. Kivshar, Observation of topological transformations of optical vortices in two-dimensional photonic lattices, *Opt. Express* **14**, 8317 (2006).
- [37] T. J. Kippenberg, A. L. Gaeta, M. Lipson, and M. L. Gorodetsky, Dissipative Kerr solitons in optical microcavities, *Science* **361**, 567 (2018); C. P. Jisha, Y. Y. Lin, T. D. Lee, and R. K. Lee, Crescent waves in optical cavities, *Phys. Rev. Lett.* **107**, 183902 (2011).

Supplementary Material for *Stable multi-ring and rotating solitons in two-dimensional spin-orbit coupled Bose-Einstein condensates with a radially-periodic potential*

Yaroslav V. Kartashov^{1,2} and Dmitry A. Zezyulin³

¹ *ICFO-Institut de Ciències Fotoniques, The Barcelona Institute of Science and Technology, 08860 Castelldefels (Barcelona), Spain*

² *Institute of Spectroscopy, Russian Academy of Sciences, Troitsk, Moscow, 108840, Russia*

³ *ITMO University, St. Petersburg 197101, Russia*

Physical units

Assuming tight harmonic confinement along the Z axis, we start with a two-dimensional Gross-Pitaevskii equation for a disk-shaped condensate in the horizontal (X, Y) plane (see e.g. [S1, S2]):

$$i\hbar \frac{\partial \Psi_{\pm}}{\partial T} = -\frac{\hbar^2}{2m} \left(\frac{\partial^2}{\partial X^2} + \frac{\partial^2}{\partial Y^2} \right) \Psi_{\pm} + 2V_0 \cos^2(R/R_0) \Psi_{\pm} \pm \frac{\gamma \hbar^2 k}{m} \left(\frac{\partial}{\partial X} \mp i \frac{\partial}{\partial Y} \right) \Psi_{\mp} + U(|\Psi_{\pm}|^2 + |\Psi_{\mp}|^2) \Psi_{\pm}. \quad (\text{S1})$$

Here T is time; X, Y are the spatial coordinates, $R^2 = X^2 + Y^2$; $2V_0$ is the potential depth, R_0 is the characteristic spatial scale (πR_0 determines diameter of the ring, where first minimum of the potential is achieved); m is the atomic mass; k is the wavenumber of lasers creating spin-orbit coupling; γ is the dimensionless coefficient depending on the particular laser scheme creating spin-orbit coupling [S2, S3]. We consider the case when the s -wave scattering lengths between atoms in the two hyperfine states are equal. Then the interactions between atoms can be described by a single coefficient U , which for a disk-shaped condensate with dimensional wavefunction Ψ_{\pm} normalized as $\iint_{-\infty}^{\infty} (|\Psi_{+}|^2 + |\Psi_{-}|^2) dXdY = 1$ has the form (see e.g. [S4])

$$U = 2aN \sqrt{\frac{2\pi \hbar^3 \omega_Z}{m}}, \quad (\text{S2})$$

where a is the s -wave scattering length, N is the total number of atoms, and ω_Z is the frequency of tight confinement along the Z axis. Next, we introduce dimensionless spatial variables

$$x = X/R_0, \quad y = Y/R_0, \quad r = R/R_0, \quad (\text{S3})$$

as well as characteristic energy \mathcal{E}_0 and dimensionless time as

$$\mathcal{E}_0 = \hbar^2/mR_0^2, \quad t = (\mathcal{E}_0/\hbar)T, \quad (\text{S4})$$

and obtain Eqs. (1) of the main text

$$i\partial_t \psi_{\pm} = -(1/2)(\partial_x^2 + \partial_y^2) \psi_{\pm} + V(r) \psi_{\pm} \pm \beta(\partial_x \mp i\partial_y) \psi_{\mp} + \sigma(|\psi_{\pm}|^2 + |\psi_{\mp}|^2) \psi_{\pm}, \quad (\text{S5})$$

where dimensionless potential depth $V_0 = V_0/\mathcal{E}_0$ is used; the strength of spin-orbit coupling $\beta = \gamma k R_0$; the parameter $\sigma = \text{sign } a$; and dimensionless spinor wavefunction $\psi_{\pm} = |U/\mathcal{E}_0|^{(1/2)} \Psi_{\pm}$ is introduced. For characteristic spatial scale of $R_0 = 2 \mu\text{m}$ (that gives diameter $6.28 \mu\text{m}$ of the first circular minimum of potential), one obtains characteristic time scale of 5.45 ms (for ^{87}Rb) or 0.44 ms (for ^7Li). Thus, for typical dimensionless rotation frequency $\omega = 0.25$ of the states from Figs. 3, 4, 6 of the main text, one rotation occurs on ~ 137 ms for ^{87}Rb and ~ 11 ms for ^7Li , i.e., the rotations times are below experimentally available lifetime of the condensate.

Equations for linear stability analysis and numerical methods

In order to address linear stability of radially-symmetric vortex modes $u_{\pm}(r)$, we use the standard substitution for slightly perturbed stationary solution:

$$\psi_{\pm}(x, y, t) = e^{-i\mu t + im_{\pm}\theta} [u_{\pm}(r) + w_{\pm,q}(r) e^{i\lambda t + iq\theta} + z_{\pm,q}^*(r) e^{-i\lambda^* t - iq\theta}], \quad (\text{S6})$$

where $w_{\pm,q}$, $z_{\pm,q}$ are small radial perturbations, and integer $q = 0, 1, 2, \dots$ is the azimuthal perturbation index. Spectrum of λ determines the growth rate of an eventual instability (the instability corresponds to λ with nonzero imaginary part). Substituting (S6) into dimensionless GPE and retaining only the terms linear in $w_{\pm,q}$ and $z_{\pm,q}$, after straightforward calculations, for each azimuthal index q , we arrive to the linear eigenvalue problem $L_q \mathbf{Z}_q = \lambda \mathbf{Z}_q$, where $\mathbf{Z}_q = (w_{+,q}, z_{+,q}, w_{-,q}, z_{-,q})^T$, and differential operator L_q has the form

$$\begin{pmatrix} M(m_+ + q) - 2\sigma u_+^2 - \sigma u_-^2 & -\sigma u_+^2 & -\sigma u_+ u_- - B(m_+ + q) & -\sigma u_+ u_- \\ \sigma u_+^2 & -M(m_+ - q) + 2\sigma u_+^2 + \sigma u_-^2 & \sigma u_+ u_- & \sigma u_+ u_- + B(-m_+ - q) \\ -\sigma u_+ u_- - B(-m_+ - q) & -\sigma u_+ u_- & M(m_- + q) - 2\sigma u_-^2 - \sigma u_+^2 & -\sigma u_-^2 \\ \sigma u_+ u_- & \sigma u_+ u_- - B(q - m_+) & \sigma u_-^2 & -M(m_- - q) + 2\sigma u_-^2 + \sigma u_+^2 \end{pmatrix},$$

where we have introduced the following notations

$$M(q) = \frac{1}{2} \left(\frac{\partial^2}{\partial r^2} + \frac{1}{r} \frac{\partial}{\partial r} - \frac{q^2}{r^2} \right) + \mu - V(r), \quad B(q) = \beta \left(\frac{\partial}{\partial r} + \frac{q}{r} \right). \quad (\text{S7})$$

The obtained linear eigenvalue problem can be solved for various q values using standard numerical finite-difference methods. In our work, we have considered the azimuthal indexes in the range $q = 0, 1, \dots, 10$.

Nonlinear stability of radially-symmetric and rotating states was also analyzed by means of direct integration of the time-dependent Gross-Pitaevskii equation (1) from the main text. The initial conditions were chosen in the form of slightly perturbed (by random or regular perturbations) exact soliton states. The time-dependent equation was solved with a split-step Fourier method, where the spatial differential operators were approximated using the fast Fourier transforms.

-
- [S1] S. Sinha, R. Nath, and L. Santos, Trapped two-dimensional condensates with synthetic spin-orbit coupling, *Phys. Rev. Lett.* **107**, 270401 (2011).
[S2] Y. Zhang, L. Mao, and C. Zhang, Mean-field dynamics of spin-orbit-coupled Bose-Einstein condensates, *Phys. Rev. Lett.* **108**, 035302 (2012).
[S3] Y. J. Lin, K. Jiménez-García, and I. B. Spielman, Spin-orbit-coupled Bose-Einstein condensates, *Nature* **471**, 83 (2011).
[S4] L. D. Carr, M. J. Holland, and B. A. Malomed, Macroscopic quantum tunnelling of Bose-Einstein condensates in a finite potential well, *J. Phys. B: At. Mol. Opt. Phys.* **38**, 3217 (2005).